

Journal of Materials Chemistry B

Accepted Manuscript



This is an *Accepted Manuscript*, which has been through the Royal Society of Chemistry peer review process and has been accepted for publication.

Accepted Manuscripts are published online shortly after acceptance, before technical editing, formatting and proof reading. Using this free service, authors can make their results available to the community, in citable form, before we publish the edited article. We will replace this *Accepted Manuscript* with the edited and formatted *Advance Article* as soon as it is available.

You can find more information about *Accepted Manuscripts* in the [Information for Authors](#).

Please note that technical editing may introduce minor changes to the text and/or graphics, which may alter content. The journal's standard [Terms & Conditions](#) and the [Ethical guidelines](#) still apply. In no event shall the Royal Society of Chemistry be held responsible for any errors or omissions in this *Accepted Manuscript* or any consequences arising from the use of any information it contains.

Charge-tunable absorption behavior of DNA on graphene

Zhe Kong¹, Wei Zheng², Qi Wang³, Hongbo Wang⁴, Fengna Xi⁵, Lijun Liang^{3, 6, *}, Jia-Wei Shen^{2, *}

¹College of Materials and Environmental Engineering, Hangzhou Dianzi University, Hangzhou, 310018, People's Republic of China

²School of Medicine, Hangzhou Normal University, Hangzhou 310016, People's Republic of China

³Soft Matter Research Center and Department of Chemistry, Zhejiang University, Hangzhou 310027, People's Republic of China

⁴College of Automation, Hangzhou Dianzi University, Hangzhou, 310018, People's Republic of China

⁵Department of Chemistry, Zhejiang Sci-Tech University, Hangzhou, Zhejiang 310018, China

⁶Department of Polymer Science and Engineering, Zhejiang University, Hangzhou 310027, People's Republic of China.

* Corresponding authors.

Fax: +86 571 87951895.

E-mail addresses:

michael.lijunl@gmail.com (L.J. Liang)

shen.jiawei@hotmail.com (J.-W. Shen)

Abstract

Solving **the problem of DNA sticking to graphene** is very important for the use of **graphene** on DNA sequence or other DNA sensor technology. In this study, we **use molecular dynamics simulation** to demonstrate that DNA tends to adsorb on pristine **neutralized graphene rather than on** graphene with negative charge. Property of graphene could be charge-tuned from DNA-philic to DNA-phobic, **and the property is** evaluated by the contact angle of DNA absorbed on graphene surface. With negative charge, graphene is prone to DNA-phobic; **with positive charge or without charge, it is likely to be DNA-philic**. The translocation time of DNA on graphene nanopore was greatly extended, if the graphene nanopore **is functionalized** by the negative charge. **This study** could help us to better design a promising device for DNA sequence by graphene nanopore.

Keywords: graphene nanopore, contact angle, molecular dynamics simulation, DNA sequence

1. Introduction

Nanopores, such as solid-state and biological¹¹⁻¹⁵ nanopores, have been proved very promising for probing single molecules. A DNA or RNA molecule driven by electric field to thread a solid-state nanopore could be directly read off by the transient ionic current. It is considered as an effective method to detect DNA sequences by nanopores with **high-efficiency**, low-cost and high-throughput.¹⁶ The unique properties and structure of graphene nanopore, especially the single-atomic thickness, **make it a unique solid-state nanopore** to detect DNA sequence. **Consequently, nanoporous material** has opened up a new chapter to **understand** DNA sequence¹⁷, and has been investigated by both experimental and theoretical studies in recent years¹⁸⁻²⁰. The DNA translocation velocity could be much slower **with ion change from Li⁺ to Na⁺ in the aqueous solution**¹⁸. Aksimentiev et al **pointed** out that the DNA sequence through graphene nanopore could stop and go with applied reversible electric field²¹. Wang et al found that the resolution of DNA sequencing could be improved by using an axisymmetric graphene nanopore²⁰. **In addition, several nanopore signal detection schemes including tunneling-based electronic readout²², field-effect sensors²³ have also been proposed. These results could greatly enhance our understanding of DNA sequencing by graphene nanopore. However, even the highest-resolution nanopore devices lack the spatial resolution required for single base recognition. Very recently, Wanunu et al indicated that a crucial criterion to the success sequence of nanopores is to control the fast and stochastic nature of DNA translocation²⁴. Solving the sticking of DNA molecules to graphene has been a big challenge for successful application of graphene nanopore to the DNA sequencing^{5, 25-28}. The hydrophobic adhesion of nucleobases to graphene could have a significant effect on the ionic current measurement for DNA sequence²⁵, and it could greatly decrease the signal-to-noise ratio (SNR).**

Based on the rapid development of lithography²⁹, transmission electron microscopy³⁰ and other bottom-up growth techniques³¹, the ability of manufacturing atomic-scale graphene-based structure has been greatly improved. It gives us multiple choices to use different modified graphene nanopore to detect the sequence of DNA. In addition, Aksimentiev et al pointed out that the conformation of DNA on different charged graphene nanopore is different in their theoretical work²¹. Thus, the study of absorption behavior of DNA on the graphene nanopore with different charge is necessary but such information is less concerned, and it is much helpful for the application of graphene nanopore as biosensor on DNA sequencing.

Besides experiments, molecular dynamics (MD) simulation has been extensively used to study the absorption behavior of the biological molecules on inorganic materials in our group³²⁻³⁴ and other groups^{35, 36}. Herein, to investigate the absorption behavior of DNA on graphene with different charge density, DNA molecule composed of 5'-

AAAAACCCCTTTTTGGGG-3' was studied for its simplicity but with all four nucleotides. To check the effect of graphene with different charge density on DNA translocation, poly(A)₁₀ was used for its simplicity. In our simulations, the absorption behavior of graphene could be changed from DNA-philic to DNA-phobic with the change of the charge on the graphene surface. The translocation time of DNA molecules to thread graphene nanopore was greatly extended in graphene nanopore with negative charge compare with that in neutralized graphene nanopore in our simulation, which is consistent with the results from the experiment³⁷.

2. Simulation details

2.1 System setup

The graphene sheet with the size of 84.8 Å × 83.7 Å was in the *x-y* plan with the center of mass in the origin (0, 0, 0) of the Cartesian coordinate. It was modified with different charge density varied from $\sigma = -3 \text{ e/nm}^2$ to $+3 \text{ e/nm}^2$. DNA molecule with the sequence of 5'-AAAAACCCCTTTTTGGGG-3' was constructed by using the Hyperchem software (Version 7.0, Hypercube, Inc), and it was equilibrated by 1 ns in vacuum. Then, DNA molecule was solvated by TIP3P water molecules³⁸, and the system underwent a 500000-step energy minimization. After that, DNA molecules was placed on the graphene with different charge varied from $\sigma = -3 \text{ e/nm}^2$ to $+3 \text{ e/nm}^2$, and TIP3P water molecules was added into the box with a density of 1.001 g/cm³. At last, Na⁺ or Cl⁻ ions were added into the solution to neutralize the system. In most cases, the water box is 85.5×84.4×90.0 Å³ in the *x*, *y* and *z* directions, as shown in Fig. 1A.

Graphene nanopores were constructed by deleting the atoms with their coordinates satisfying $x^2+y^2 < R^2$, where *R* is radius of the graphene nanopore and it is 20Å in this study. It was modified with different charge density varied from $\sigma = -3 \text{ e/nm}^2$ to $+3 \text{ e/nm}^2$. Poly(A)₁₀ was constructed by using the Hyperchem software (Version 7.0, Hypercube, Inc). The nanopores and poly(A)₁₀ were solvated in a box with TIP3P water molecules and the system underwent a 500000-step energy minimization. Then, NaCl ions were added to match the desired concentrations. In most cases, the water box is 60.0×60.0×160.0 Å³ in the *x*, *y* and *z* directions, as shown in Fig.1B and 1C.

2.2 System Simulation

All simulations were performed by Gromacs-4.5.3 program with the time step of 2 fs. The DNA molecule, Na⁺ and Cl⁻ ions were modeled by the Charmm27 force field. The force field parameters of carbon atoms in graphene were $\sigma_{CC} = 3.85 \text{ \AA}$ and $\epsilon_{CC} = -0.439 \text{ kcal/mol}$ as used in previous work³⁹. All atoms including hydrogen atoms were represented explicitly, and the bonds with hydrogen atom were constrained. The cutoff for the non-bonded van der Waals

interaction was set by a switching function starting at 10 Å and reaching zero at 12 Å. The Langevin method was employed to keep the temperature at 298 K and the pressure at 101.3 kPa. In the systems of simulating translocation of DNA through graphene nanopore, the electric field with $E = 100$ mv/nm was used.

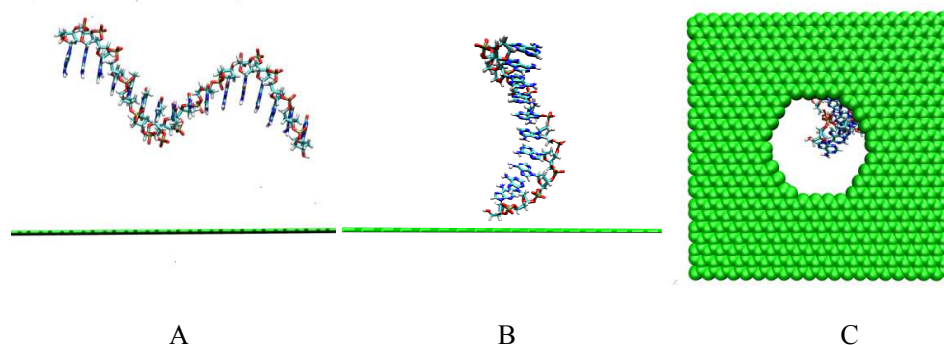


Fig. 1 (A): The system for absorption of DNA on graphene sheet. The initial structure of DNA molecule (5'-AAAACCCCTTTTGGGG-3') on the graphene sheet; (B) side view and (C) top view of the system of simulating DNA translocation through graphene nanopore. The water molecules and ions are not shown for clarity. The atoms colored green are graphene, and nucleotides are shown by licorice mode.

2.3 Analysis method

Calculation of contact angle

The calculation of contact angle of DNA molecules on the graphene sheet was similar to the methods for calculation of contact angle of water molecules on graphene sheet as used in reference⁴⁰. The MD trajectory in the last 5 ns was analyzed to calculate the contact angle. Firstly, the z -axis was defined through the center of mass of the DNA molecule. Secondly, the system was divided into cubic meshes with each mesh has spatial dimensions of $0.5 \times 0.5 \times 0.5$ Å³. The number of DNA atoms in each mesh is calculated, and all the meshes contain more than one DNA atoms were recorded. For a selected layer of meshes (in parallel with graphene sheet), due to the irregular geometry of layer mesh of DNA molecule on graphene, the DNA atoms with the largest distance in positive and negative directions of x and y to the center of mass of DNA atoms were denoted as $d(x^+)_{\max}$, $d(x^-)_{\max}$, $d(y^+)_{\max}$, and $d(y^-)_{\max}$, and the average value $R(z)$ of these four number was calculated as the radius of this mesh. Thirdly, all the radius values along with the height of z axis were calculated. At last, the contact angle (θ) was measured based on the fitting by equation (1) (A , B , and C are constants).

$$R(z) = Az^2 + Bz + c. \quad (1)$$

Herein, the contact angle of DNA on the graphene larger than 90° is defined as DNA-phobic⁴¹, which indicates strong interaction between DNA and graphene; otherwise, it will

be defined as DNA-philic if the contact angle is smaller than 90° , which imply relative weak interaction between DNA and graphene⁴¹.

Calculation of translocation time

The translocation time Δt_{tl} of a DNA fragment through a nanopore was calculated as our previous work⁴²

$$\Delta t_{tl} = t_2 - t_1 \quad (2)$$

where t_1 is the time when the first atom of the DNA fragment enters into the nanopore and t_2 is the time when the DNA fragment exits the nanopore completely. All DNA atoms were tracked with their positions; therefore, one could track the first atom that enters into the nanopore as well as the time t_1 . Similarly, if all atoms translocate through the position of graphene nanopore, t_2 could be identified.

3. Results and discussion

3.1 Charge-tunable absorption behavior of DNA on graphene

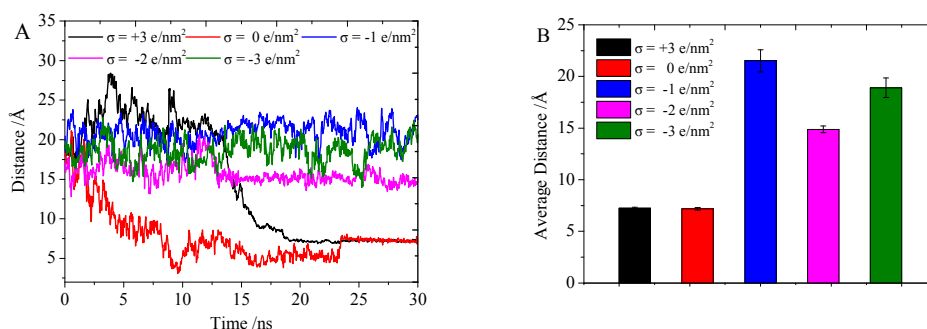


Fig. 2 The distance of center-of-mass of DNA molecule from the surface of graphene with varied charged density: (A) along with the simulation time; (B) the average distance in the last 5 ns of simulations.

As shown in Fig. 2A, **the distance between** the center-of-mass (COM) of DNA molecule and that of graphene with different charge densities was measured in all simulations. **The initial distance between the COM of DNA molecule and that of graphene is 20 Å. As can be seen in the schematic in Fig.S1 (see the supporting information), with the existence of the PBC, the strong interaction between DNA and +3 charged surface lead DNA to be absorbed on the image layer of graphene in z direction. Therefore, the distance between DNA and graphene with the charge density of $\sigma = +3 \text{ e/nm}^2$ fluctuated much in the first 10ns. With the effect of thermal fluctuation and strong absorption of graphene**

layer, the DNA molecule finally absorbed on the graphene layer after 15 ns in simulation.

In the system with the charge density from $\sigma = +3 \text{ e/nm}^2$ to $\sigma = 0 \text{ e/nm}^2$, the distance decreased sharply **at last 5 ns** due to the strong absorption of DNA to graphene sheet. The average distance in these two systems in the last 5 ns is ca. 7.5 \AA , as seen in Fig. 2B. However, the distance didn't dramatically decreases in other three systems with charge density varied from $\sigma = -1 \text{ e/nm}^2$ to $\sigma = -3 \text{ e/nm}^2$. As seen in Fig. 2B, the average distance is 21.5, 14.8, and 19.1 \AA in the systems with the charge density $\sigma = -1 \text{ e/nm}^2$, -2 e/nm^2 and -3 e/nm^2 in the last 5ns. These results indicate that the DNA molecule could be adsorbed on the graphene with no charge or with positive charge but not with negative charge. The interaction between DNA molecule and graphene with different charge density was measured in the last 5 ns. As displayed in Fig. 3A, the interaction between DNA and graphene with $\sigma = +3 \text{ e/nm}^2$ is the largest, which is ca. -1480.2 kJ/mol . The second largest one is the interaction between DNA and graphene with $\sigma = 0 \text{ e/nm}^2$, and it is around -1350.3 kJ/mol . The interaction between DNA and graphene in other three systems with negative charge is very small, especially in the system of graphene with $\sigma = -3 \text{ e/nm}^2$, and it is close to 0 kJ/mol . The electrostatic energy of DNA and graphene with negative charge is so small ($< 10 \text{ kJ/mol}$, **see in Fig.S2 in supporting information**) that it could hardly be displayed in the Fig. 3A. The interaction energy between DNA and graphene with $\sigma = +3 \text{ e/nm}^2$ is smaller than that of DNA with no charge graphene. The reason is that the van der Waals (vdW) interaction energy between graphene (**with $\sigma = +3 \text{ e/nm}^2$**) and DNA was much smaller than that of DNA and graphene with no charge. As the π - π stacking interaction has been proved to play a significant role in DNA-graphene interaction, we carefully checked the average number of π - π stacking interaction between the base of nucleotide and graphene. Here we made the two criteria of forming π - π stacking interaction between the nucleotide and graphene⁴³: (1) the angle between the plane of base of nucleotide and plane of graphene sheet is smaller than 10° ; (2) the distance between the center-of-mass of base and graphene sheet is less than 5 \AA . Fig. 3B shows the average number of π - π stacking interaction between nucleotides and graphene, calculated from last 5 ns of simulations. The number of π - π stacking interaction between nucleotides and graphene without charge is 6.0, and it is 2.8 in the system with $\sigma = +3 \text{ e/nm}^2$. It indicates that the π - π stacking interaction between DNA and positively charged graphene was much weaker than that in the system of graphene without charge. In the system of graphene without charge, the strong van der Waals interaction which mainly contributed by π - π stacking interaction leads to strong adsorption of DNA on the graphene sheet, and DNA-graphene system tend to reach the most stable configuration and lowest energy by adopt the parallel orientation of bases to graphene. However, the strong electrostatic energy between negatively charged DNA molecule and graphene with positive charge could affect the conformation of DNA molecule absorbed on graphene sheet. The DNA molecule prefers to

interact with positively charged graphene via negatively charged phosphate groups. The consequence is that most of the bases of nucleotide could not achieve the orientation that parallel to positively charged graphene sheet, and the distance between center-of-mass of nucleotides and positively charged graphene is much longer than that between nucleotides and graphene without charge. The number of nucleotides forming π - π stacking interaction with graphene is even less in the system of negatively charged graphene, especially in the system of graphene with $\sigma = -3 \text{ e/nm}^2$. The strong electrostatic energy between negatively charged DNA molecule and negatively charged graphene could extensively repel DNA molecules from graphene sheet. That is also the reason that the distance between DNA molecule and graphene with negative charge is very large, as seen in Fig. 2B. To interpret the difference of absorption behavior of DNA on graphene with different charge more intuitively, the contact angle of DNA molecule on the graphene sheet was calculated (Details were described in section 2.3). The measured contact angle is sensitive to the height of the plane. Based on the methods from reference³⁷, the first peak position of the density profile in the z direction (black dash line) is defined as $z=0$ for the contact angle measures. As shown in Fig. 4A, the contact angle is the angle between two black dashed lines, which is bases on the fitted equation of radius of slab in z direction (red line).

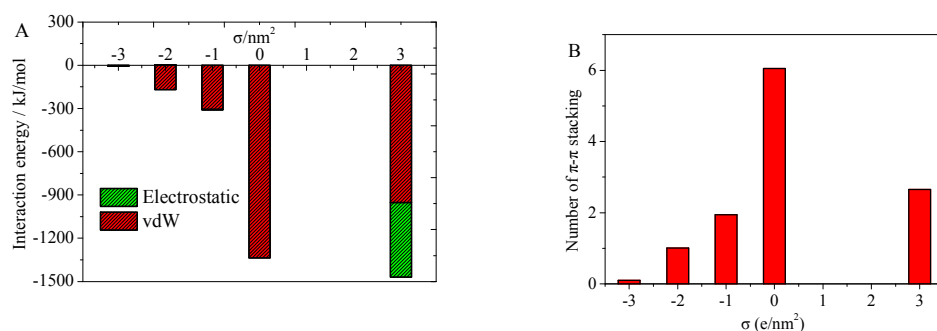


Fig. 3 (A). Interaction between DNA molecule and graphene with different charge density varied from $\sigma = +3 \text{ e/nm}^2$ to $\sigma = -3 \text{ e/nm}^2$ is calculated from last 5 ns of simulations. Red is the van der Waals (vdW) interaction and green is the electrostatic interaction. **The electrostatic energy between DNA and graphene with different charge density varied from $\sigma = -1 \text{ e/nm}^2$ to $\sigma = -3 \text{ e/nm}^2$ is too small to seen in this figure, and the detail is seen in Fig. S2 (supporting information).** (B) The number of π - π stacking interaction between nucleotides and graphene is measured in the last 5 ns with the criteria that the distance of center mass of DA is less than 5 \AA to the graphene and the angle of plane of nucleotide to graphene is less than 10 degree.

In the system of graphene without charge, the contact angle of DNA on the graphene is ca. 45.1° , and it is ca. 151.2° in the system of graphene with $\sigma = -3 \text{ e/nm}^2$. It indicate that DNA

tends to be adsorbed on the neutral graphene sheet, but not on the graphene with $\sigma = -3 \text{ e/nm}^2$. As shown in Fig. 4B, the contact angle decreases from 151° to 30° with the change of charge on the graphene varied from $\sigma = -3 \text{ e/nm}^2$ to $\sigma = +3 \text{ e/nm}^2$. It implied that the property of graphene that adsorb DNA molecule has been changed from DNA-philic to DNA-phobic with the change of the charge in graphene surface from positive to negative. The neutral graphene is DNA-philic since the contact angle is 45° , which is smaller than 90° . It means that neutral graphene could strongly interact with DNA, which is in consistence with the results from experiment⁴⁴ and theoretical works⁴⁵. It is also the reason that DNA stick on the graphene surface in DNA sequencing by graphene nanopore^{46, 47}. It implies that the DNA will not adhere to graphene surface by modifying the surface charge of graphene to be negative. In addition, the distance between the DNA and graphene with $\sigma = -3 \text{ e/nm}^2$ is much longer than that of DNA and graphene with the charge $\sigma = +3 \text{ e/nm}^2$. In the system of graphene with negative charge, the Na^+ ion could be absorbed strongly on the graphene. To investigate the distribution of Na^+ ion on the graphene with different charge, the density profiles of Na^+ in the z direction were calculated. The total number of Na^+ ions in different system is different, thus, the value showed in the Fig. 4C is the normalized density distribution in z direction. The first peak of density profile of Na^+ in the z direction in graphene with $\sigma = -3 \text{ e/nm}^2$ is about 16, which is much higher than the first peak in other two systems. In other two systems with neutral or positively charged graphene sheets, the first peaks are 2.1 and 0.7, respectively. The interesting thing is that the first peak of Na^+ ions is much higher than the second peak (1.6) in system with negatively charged graphene sheet, but is not in other systems. Strong electrostatic interaction drive Na^+ but not DNA molecule absorbed on the graphene with $\sigma = -3 \text{ e/nm}^2$.

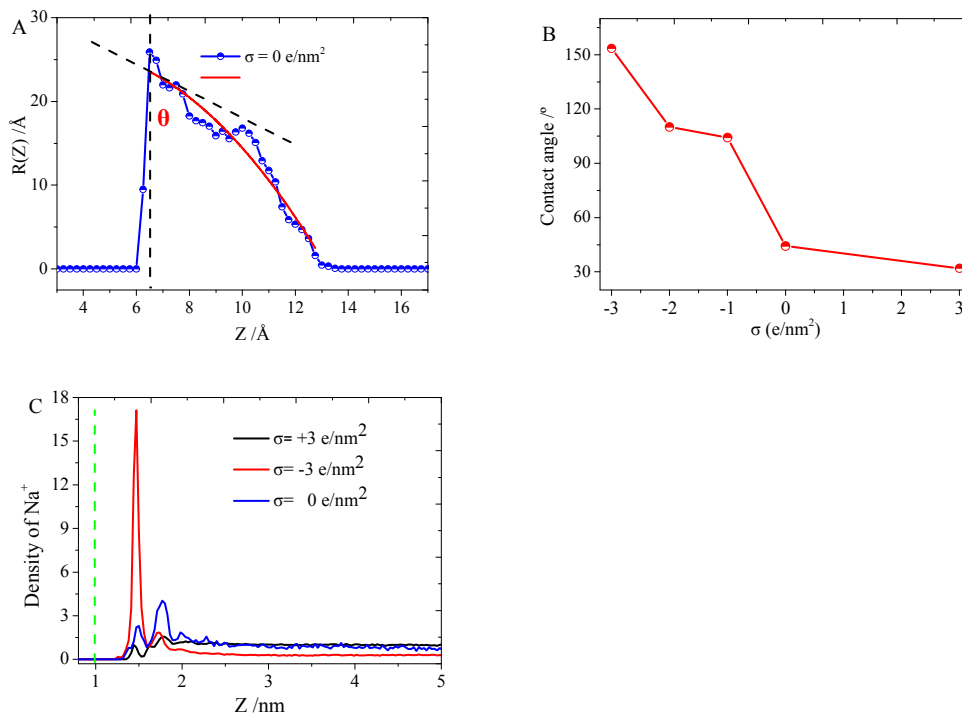


Fig. 4 (A) Illustration of the contact angle measurements based on the simulation. The blue circle line is composed of the radius of the slabs in the z direction, which is the average value of four largest distance of DNA atoms in positive and negative directions of x and y to the center of mass of DNA atoms. The red curve marks the fitted surface of the DNA molecule on the graphene. The contact angle (θ) is the angle between the (black) tangent dashed line and the xy plane (marked by the vertical black dashed line). (B) The contact angle of DNA on the graphene with different charge density varied from $\sigma = +3 \text{ e/nm}^2$ to $\sigma = -3 \text{ e/nm}^2$. (C) The normalized density of Na^+ on the z direction of graphene with different charges. The green dash line is the location of graphene in the z direction.

3.2 Slowing DNA translocation of DNA through graphene nanopore

To check the effect of graphene with different charge density on DNA translocation dynamics and DNA sequencing, the poly(A)₁₀ was used for simplicity. As seen in Fig. 5A, the translocation time of poly(A)₁₀ in graphene nanopore with different charge varied from $\sigma = +3 \text{ e/nm}^2$ to $\sigma = -3 \text{ e/nm}^2$ is calculated under electric field of 100 mv/nm. With the charge density of graphene nanopore change from $\sigma = +3 \text{ e/nm}^2$ to $\sigma = -3 \text{ e/nm}^2$, the translocation time for poly(A)₁₀ is increased from 0.51 ns to 5.52 ns. It shows that the DNA translocation through graphene nanopore slowed down with charge density change from positive to negative. **The simulation results is confirmed by the results from experiments, where Meller et al. found that the DNA translocation time could be extended 10 times or more by using negatively charged graphene nanopore³⁷. However, different from the results in**

Fig.3A, the vdW interactions between poly(A)₁₀ and graphene nanopores in the translocation process were less affected with change of the charge density of graphene nanopore, as shown in Fig. 5B. The vdW interaction between DNA and graphene surface could be affected greatly by the distance of DNA from the graphene surface. In the DNA translocation process, DNA was strongly driven to pass through the graphene nanopore with charge or without charge by applied bias electric field. Thus, the distance of DNA molecule to graphene nanopore with different charge was very small and could only change a little since DNA needs to translocate through nanopore. The vdW interaction between DNA and graphene could only change a little when the graphene nanopore was modified by different charges. However, the electrostatic energy between poly(A)₁₀ and graphene nanopore could change dramatically. The electrostatic energy between poly(A)₁₀ and graphene nanopore increases from -359.2 kJ/mol to 328.1 kJ/mol with the change of charge density on graphene nanopore varied from $\sigma = +3 \text{ e/nm}^2$ to $\sigma = -3 \text{ e/nm}^2$. The high electrostatic energy between poly(A)₁₀ and negatively charged graphene nanopore could repel poly(A)₁₀ when it is in the graphene nanopore. As a result of increase of electrostatic energy, the poly(A)₁₀ translocation time was extended. In addition, the structure of poly(A)₁₀ could be affected extensively in graphene nanopore with the change of the charge density. Fig. 6 shown the stretching of poly(A)₁₀ during the translocation process. For simplicity, the average distance between four nucleotides with one in the nanopore is calculated in the DNA translocation process. The distance of these bases in the graphene nanopore with charge density of $\sigma = -3 \text{ e/nm}^2$ (Fig.6A), $\sigma = 0 \text{ e/nm}^2$ (Fig.6B) and $\sigma = +3 \text{ e/nm}^2$ (Fig.6C) are shown in Fig.6. The average distance between four nucleotides in initial structure of poly(A)₁₀ is ca. 19.77 Å. It extended to 21.16 Å when DNA is in the translocation process in the system of graphene nanopore with $\sigma = -3 \text{ e/nm}^2$. The distance is much shorter in the systems of graphene nanopore without charge and positive charge. Especially, it is only 15.55 Å in the system of graphene nanopore with $\sigma = +3 \text{ e/nm}^2$, which imply that poly(A)₁₀ has condensed much. The snapshots of distance between four nucleotides in graphene nanopore with different charge density reveal that poly(A)₁₀ is strongly repelled by negatively charged graphene nanopore and it extensively stretched. However, the structure of poly(A)₁₀ condenses a little due to the attraction between poly(A)₁₀ and graphene nanopore without charge or positive charge. **In the view of the simplicity of poly(A)₁₀, the DNA translocation process using the complex DNA molecule composed of four different types of nucleotides will be investigated in graphene nanopore modified by different charge in future.**

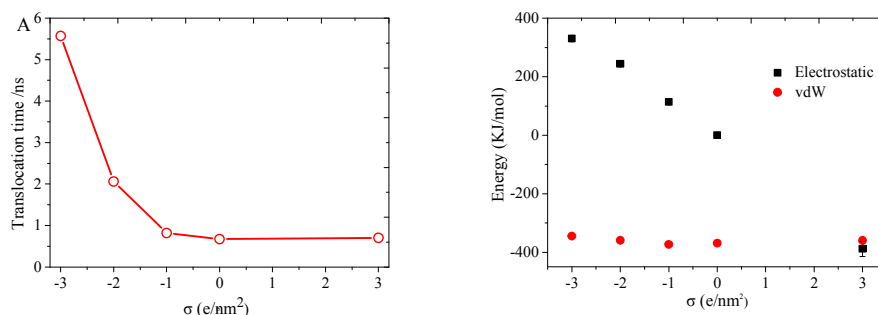


Fig.5 (A) The change of poly(A)₁₀ translocation time through graphene nanopore with different charge density varied from $\sigma = +3 e/nm^2$ to $\sigma = -3 e/nm^2$; (B) The interaction between poly(A)₁₀ and graphene nanopore with different charge density varied from $\sigma = +3 e/nm^2$ to $\sigma = -3 e/nm^2$. The black square is the electrostatic energy, and the red circle is vdW energy.

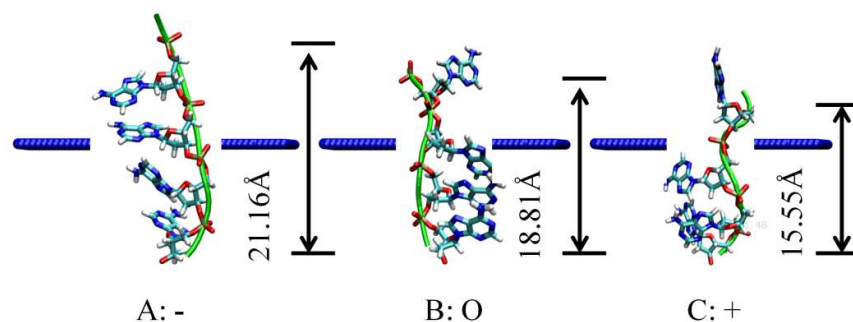


Fig.6 The stretching of poly(A)₁₀ through graphene nanopore with different charge density varied from $\sigma = -3 e/nm^2$ (A: -), $\sigma = 0 e/nm^2$ (B: O) and $\sigma = +3 e/nm^2$ (C: +). For simplicity, only 4 nucleotides of poly(A)₁₀ were shown in the snapshots. The blue van der Waals model represent the graphene nanopore, and the nucleotides are represent by tube and licorice model.

4. Conclusion

In this study, the absorption of DNA on the graphene with varied charged density was studied via molecular dynamics simulation. DNA tends to adsorb on the pristine neutral graphene by π - π stacking interaction with the plane of nucleotide parallel to graphene. In the system of graphene with negative charge, DNA could not adsorb on graphene, and the interaction between DNA and graphene is very weak. Evaluated by the contact angle of DNA on graphene surface, we demonstrate that graphene could be tuned from DNA-philic to DNA-phobic with different charge density on the surface. With negative charge, graphene is DNA-phobic, and it is DNA-philic with no charge or with positive charge. In addition, our simulation shows that the DNA translocation could be slowed down in the graphene nanopore with negative charge. These results may help to better understand the interaction between

DNA and graphene at the molecular level and design a promising device for DNA sequencing by using graphene nanopore.

Acknowledgment

J.-W. Shen gratefully acknowledges financial support by the National Natural Science Foundation of China (Grant Nos. 21403049), Zhejiang Provincial Natural Science Foundation of China (Grant Nos. LY14B030008) and start funding of Hangzhou Normal University (Nos. PE13002004041). Z. Kong gratefully acknowledges financial support by the Zhejiang Provincial Natural Science Foundation of China (Grant Nos. LY15E030009 and Nos. LY13F040006) and the Science and Technology Project of Zhejiang Province (Nos. 2014C33220).

References

1. B. Q. Luan, H. B. Peng, S. Polonsky, S. Rosnagel, G. Stolovitzky and G. Martyna, *Phys. Rev. Lett.*, 2010, **104**.
2. B. Q. Luan, G. Martyna and G. Stolovitzky, *Biophys. J.*, 2011, **101**, 2214-2222.
3. J. L. Li, M. Gershow, D. Stein, E. Brandin and J. A. Golovchenko, *Nat. Mater.*, 2003, **2**, 611-615.
4. V. Mussi, P. Fanzio, L. Repetto, G. Firpo, P. Scaruffi, S. Stigliani, G. P. Tonini and U. Valbusa, *Nanotechnology*, 2010, **21**.
5. B. Q. Luan, G. Stolovitzky and G. Martyna, *Nanoscale*, 2012, **4**, 1068-1077.
6. J. L. Li, D. Stein, C. Qun, E. Brandin, A. Huang, H. Wang, D. Branton and J. Golovchenko, *Biophys. J.*, 2003, **84**, 134a-135a.
7. A. J. Storm, J. H. Chen, X. S. Ling, H. W. Zandbergen and C. Dekker, *Nat. Mater.*, 2003, **2**, 537-540.
8. A. J. Storm, C. Storm, J. H. Chen, H. Zandbergen, J. F. Joanny and C. Dekker, *Nano Lett.*, 2005, **5**, 1193-1197.
9. D. Fologea, J. Uplinger, B. Thomas, D. S. McNabb and J. L. Li, *Nano Lett.*, 2005, **5**, 1734-1737.
10. C. Dekker, *Nat. Nanotechnol.*, 2007, **2**, 209-215.
11. T. Z. Butler, J. H. Gundlach and M. A. Troll, *Biophys. J.*, 2006, **90**, 190-199.
12. R. F. Purnell and J. J. Schmidt, *ACS Nano*, 2009, **3**, 2533-2538.
13. D. Stoddart, G. Maglia, E. Mikhailova, A. J. Heron and H. Bayley, *Angew. Chem. Int. Edit.*, 2010, **49**, 556-559.
14. L. Franceschini, E. Mikhailova, H. Bayley and G. Maglia, *Chem. Commun.*, 2012, **48**, 1520-1522.
15. D. Stoddart, A. J. Heron, E. Mikhailova, G. Maglia and H. Bayley, *P. Natl. Acad. Sci. USA*, 2009, **106**, 7702-7707.
16. J. J. Kasianowicz, E. Brandin, D. Branton and D. W. Deamer, *P. Natl. Acad. Sci. USA*, 1996, **93**, 13770-13773.
17. Z. S. Siwy and M. Davenport, *Nat. Nanotechnol.*, 2010, **5**, 697-698.
18. S. W. Kowalczyk, D. B. Wells, A. Aksimentiev and C. Dekker, *Nano Lett.*, 2012, **12**, 1038-1044.
19. L. Liang, P. Cui, Q. Wang, T. Wu, H. Ågren and Y. Tu, *RSC Adv.*, 2013, **3**, 2445-2453.

20. Z. Zhang, J. Shen, H. Wang, Q. Wang, J. Zhang, L. Liang, H. Ågren and Y. Tu, *J. Phys. Chem. Lett.*, 2014, **5**, 1602-1607.
21. M. Shankla and A. Aksimentiev, *Nat. Commun.*, 2014, **5**.
22. M. Tsutsui, M. Taniguchi, K. Yokota and T. Kawai, *Nat Nanotechnol.*, 2010, **5**, 286-290.
23. F. Traversi, C. Raillon, S. M. Benameur, K. Liu, S. Khlybov, M. Tosun, D. Krasnozhan, A. Kis and A. Radenovic, *Nat Nanotechnol.*, 2013, **8**, 939-945.
24. S. Carson and M. Wanunu, *Nanotechnology*, 2015, **26**, 074004.
25. D. B. Wells, M. Belkin, J. Comer and A. Aksimentiev, *Nano Lett.*, 2012, **12**, 4117-4123.
26. G. F. Schneider, Q. Xu, S. Hage, S. Luik, J. N. H. Spoor, S. Malladi, H. Zandbergen and C. Dekker, *Nat. Commun.*, 2013, **4**.
27. S. Garaj, S. Liu, J. A. Golovchenko and D. Branton, *P. Natl. Acad. Sci. USA*, 2013, **110**, 12192-12196.
28. H. Bayley, *Nature*, 2010, **467**, 164-165.
29. W. Zhang, Q. Zhang, M.-Q. Zhao and L. T. Kuhn, *Nanotechnology*, 2013, **24**, 275301.
30. B. Song, G. F. Schneider, Q. Xu, G. Pandraud, C. Dekker and H. Zandbergen, *Nano Lett.*, 2011, **11**, 2247-2250.
31. A. N. Sokolov, F. L. Yap, N. Liu, K. Kim, L. Ci, O. B. Johnson, H. Wang, M. Vosgueritchian, A. L. Koh and J. Chen, *Nat. Commun.*, 2013, **4**.
32. L.-j. Liang, Q. Wang, T. Wu, J.-w. Shen and Y. Kang, *Chin. J. Chem. Phys.*, 2009, **22**, 627-634.
33. J.-W. Shen, T. Wu, Q. Wang and Y. Kang, *Biomaterials*, 2008, **29**, 3847-3855.
34. L. J. Liang, T. Wu, Y. Kang and Q. Wang, *ChemPhysChem*, 2013, **14**, 1626-1632.
35. R. J. Chen, Y. Zhang, D. Wang and H. Dai, *J. Am. Ceram. Soc.*, 2001, **123**, 3838-3839.
36. B. Adhikari and A. Banerjee, *Soft Matter*, 2011, **7**, 9259-9266.
37. N. Di Fiori, A. Squires, D. Bar, T. Gilboa, T. D. Moustakas and A. Meller, *Nat. Nanotechnol.*, 2013, **8**, 946-951.
38. W. L. Jorgensen, J. Chandrasekhar, J. D. Madura, R. W. Impey and M. L. Klein, *J. Chem. Phys.*, 1983, **79**, 926-935.
39. L. J. Liang, Q. Wang, T. Wu, T. Y. Sun and Y. Kang, *ChemPhysChem*, 2013, **14**, 2902-2909.
40. H. Li and X. C. Zeng, *ACS Nano*, 2012, **6**, 2401-2409.
41. S. Cui, J. Yu, F. Kühner, K. Schulten and H. E. Gaub, *J. Am. Ceram. Soc.*, 2007, **129**, 14710-14716.
42. C. Shi, Z. Kong, T. Sun, L. Liang, J. Shen, Z. Zhao, Q. Wang, Z. Kang, H. Ågren and Y. Tu, *RSC Adv.*, 2015, **5**, 9389-9395.
43. A. K. Manna and S. K. Pati, *J. Mater. Chem. B*, 2013, **1**, 91-100.
44. N. Mohanty and V. Berry, *Nano Lett.*, 2008, **8**, 4469-4476.
45. C.-L. Cheng and G.-J. Zhao, *Nanoscale*, 2012, **4**, 2301-2305.
46. W. Lv, S. Liu, X. Li and R. a. Wu, *Electrophoresis*, 2014, **35**, 1144-1151.
47. S. Banerjee, J. Wilson, J. Shim, M. Shankla, E. A. Corbin, A. Aksimentiev and R. Bashir, *Adv. Funct. Mater.*, 2014.